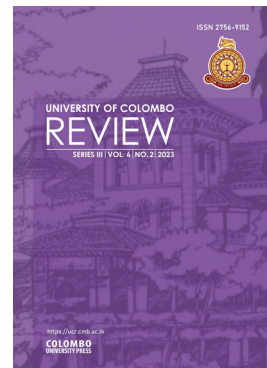


<https://doi.org/10.4038/ucr.v4i2.167>

University of Colombo Review (Series III),
Vol.4, No.2, 2023



Use of Synthetic Aperture Radar (SAR) imagery on oil spill detection: A case study on the MV X-Press Pearl container ship incident in 2021 in Sri Lanka

M.A.S. Manoj Madduma Arachchi

Faculty of Graduate Studies, University of Sri Jayewardenepura

ABSTRACT

Oil spills on the ocean from ships have a strong impact on the environment as well as on human societies. The MV X-Press Pearl container ship incident in 2021 became the worst marine environmental disaster in Sri Lanka due to its powerful impact. Oil leakage from the ship to the ocean continued for months. Synthetic Aperture Radar (SAR) imagery has the advantage of penetrating cloud cover, as well as day and night operating capabilities. Therefore, SAR imagery can be used to detect as well as observe the temporal changes of oil spills. The study in this article aimed to detect the oil spill caused by the MV X-Press Pearl container ship on Sri Lanka's west coast from May to August 2021 using Sentinel-1 SAR data and measure the temporal changes of the oil slick. Three SAR imageries with Vertical-Vertical (VV) and Vertical-Horizontal (VH) polarization from June, July, and August of 2021 have been processed by applying the orbit file, running the multi-looking algorithm, and making the ellipsoid correction. The possible oil spills have been identified from each set of imagery as dark linear shapes with lengths of 3.1 ± 0.012 km with an average reflectance of 15.6 decibels for June and 3.6 ± 0.012 km with an average reflectance of 16.5 decibels for the other two months, and the shapes correspond with the oil slick classifications from other literature. The results indicate that the VV polarization is the most suitable to detect oil spills, and that the oil spill from the X-Press Pearl continued from June to the end of August 2021.


KEYWORDS:

MV X-Press Pearl; Oil spills; Polarization; Sentinel-1; Synthetic Aperture Radar (SAR)

Suggested Citation: Madduma Arachchi, M.A.S.M. (2023). Use of Synthetic Aperture Radar (SAR) imagery on oil spill detection: A case study on the MV X-Press Pearl container ship incident in 2021 in Sri Lanka. University of Colombo Review (New Series III), 4(2), 108-125

© 2023 The Author. This work is licenced under a Creative Commons Attribution 4.0 International Licence which permits unrestricted use, distribution, and reproduction in any medium, provided the original work is properly cited.

✉ Corresponding author: manojmaddumaarachchi@gmail.com

 <https://orcid.org/0000-0003-2246-7755>

Introduction

On 19th May 2021, Singapore flagged the MV X-Press Pearl container ship anchored around 9 nautical miles (17 kilometers) northwest of the Port of Colombo in Sri Lankan national waters. On 20th May 2021, chemical fume emissions erupted on the ship (Perera & Kumudika, 2021; Partow et al., 2021). Built in 2021, this 186-meter-long ship burned for 13 days, and it has been described as the worst maritime environmental disaster in Sri Lanka's history (Rubesinghe et al., 2022; Maritime Executive, 2021). 1,486 shipping containers were on board the ship. Among those, 81 containers were carrying dangerous goods such as nitric acid, caustic soda, and methanol (Partow et al., 2021) while other containers had a mixture of several tons of potentially toxic epoxy resin, plastics, and oil, as well as metals such as lead and copper (Bozzi, 2021).

The fire and explosions that occurred on 25 May caused the containers to fall overboard and the contents of the containers to start to leak out into the ocean. Apart from the mentioned hazardous goods, the vessel contained 348 tons of bunker fuel which created the fear of a major oil spill within the region (Partow et al., 2021). An effort to drag the ship to a deeper water refuge failed and resulted in the partial sinking of the ship, and by 17 June, the entire vessel had settled on the seabed at a depth of about 21 meters. This situation led to fishing being prohibited in large areas along the coast, hundreds of dead turtles floating ashore, and tons of waste covering the western and southern coasts of Sri Lanka (Partow et al., 2021; Rubesinghe, et al., 2022).

Fears of an oil spill became a reality when an oil slick of an approximate area of 0.51 km² and a length of 3.23 km was detected near the X-Press Pearl ship on 8 June with RADARSAT 2 satellite imagery by the European Maritime Safety Agency (Partow et al., 2021). By 14 June 2021, the oil slick had expanded further, reaching a length of 4.3 km (Pallewatta et al., 2023). The United Nations Environment Program (UNEP) team who had assessed the damage of the disaster concluded that the continuous release of oil was flowing from the ship for nearly one month (8 June-4 July) (Partow et al., 2021).

An oil spill in an ocean can be harmful in many ways. It directly causes damage to the marine environment, and the communities who are utilizing the marine resources will be affected. Most families who are living in the coastal regions depend on the ocean in many ways. Therefore, the need for oil slick detection is crucial to locate polluted areas and evaluate slick drift to protect the coastline (Akkartal & Sunar, 2008).

Most oils have the propensity to spread horizontally, leaving a smooth and slick surface on top of the water. Surface tension, specific gravity, and viscosity are factors that influence how easily an oil spill can spread (Marghany, 2023). With ocean waves, oil spills can be widely spread, so observing the oil spill from the

ground is difficult. Aircraft surveillance, Side-Looking Airborne Radar (SLAR), Infrared (IR), and Ultraviolet (UV) scanners can observe these oil spills. However, these technologies have limited coverage and high operational costs (Espedal & Johannessen, 2000). Satellite imagery allows researchers to view the spill overhead with a larger view and coverage of the spill location (Kolokoussis & Karathanassi, 2018). In addition, these remote sensing methods can provide information on the rate and direction of oil movement through multi-temporal imaging. A series of satellite images and change detection approaches enhance the process of comparing the size and shape of oil spills visually and statistically (Balogun et al., 2020; Bonnington et al., 2021).

Some studies have examined optical satellite sensors for oil spill detection in the oceans (Bonnington et al., 2021; Roberto & Giovanni, 2018; Hu et al., 2021). However, optical sensors are not capable of operating during the nighttime and are affected by cloud coverage. Synthetic Aperture Radar (SAR) can overcome these difficulties and because of its day and night all-weather capabilities, it has become a very important instrument in oil spill monitoring (Marghany, 2023). The ability of SAR to detect oil slicks over the ocean surface is proven by many studies aimed at oil spill detection using SAR images (Mahindapala, 2020; Afgatiani et al., 2022; Akkartal & Sunar, 2008; Kubat et al., 1998; Martinez & Moreno, 1996).

SAR satellites gather signals in different polarizations such as V (vertical polarization) and H (horizontal polarization). A single-polarization system transmits and receives a single polarization, typically in the same direction, resulting in a horizontal-horizontal (HH) or vertical-vertical (VV) image. A dual-polarization system might transmit in one polarization but receive in two, resulting in either HH and HV or VH and VV imagery (NISAR, n.d.).

In the SAR imagery system, particularly for an oil spill, the drop of radar backscatter is referred to as the nearness of an oil slick, and it comes up as a dark region (Chaturvedi et al., 2020). The SAR imagery acquired at VV polarization is especially sensitive to the sea surface roughness. Oil spills reduce radar backscatter, and the sea surface with oil slick appears darker in the image. Therefore, some studies claimed that VV polarization is better than other polarizations for oil spill detection (Mahindapala, 2020; Natural Resources, Canada, 2015). However, Alpers et al. (2017) questioned the high success rate of oil spill detection algorithms using single-polarization because these algorithms are trained using subjective interpretation and are not validated by on-site inspections or multi-sensor measurements. Some studies like Shirvany et al. (2012) utilized dual-pol SAR over single-polarization and they suggested compact and dual-pol modes deliver better detection performance.

Even though differentiating oil and lookalikes is based on analysis of shape, size, dB-values, gradients, texture, instantaneous wind, currents, platform, ship lane, and natural seepage locations, Espedal (2010) claims that the temporal

evolution of the wind before SAR imaging also has significant influence. According to Espedal (2010), the geometrical shape of the slick is matched against wind history to estimate slick age. Pavlakis et al. (2001) classified the spills in terms of their shapes (Figure 3). The freshness of an oil spill can be determined by its shape because old spills have more complex border structures than fresh ones. The tails can be thin, straight, or slightly curved for oil spills. The roundness of dark formations is essential for identifying fresh spills, elongated with or without curves (Topouzelis, 2008).

Two dominant approaches are available for the detection of oil spills using SAR images. The first method is the manual approach where operators are trained to detect oil spills and the other method is a semi- or fully-automated approach. Manual interpretation depends on the experience of the interpreter and is performed to distinguish oil spills from look-alikes (Topouzelis, 2008).

Semi-automatic or fully automatic methodologies are more complex and they are based on the detection, isolation, and extraction of possible oil spills using thresholding and segmentation processing (Topouzelis, 2008).

Solberg et al. (2007) have produced algorithms for the automatic detection of oil spills using Radarsat and Envisat SAR images. These algorithms were produced by training those SAR images to detect, extract, and classify dark spots as oil spills or look-alikes. Solberg et al. (1999) also tested statistical modeling with a rule-based approach to automatic detection of oil spills in SAR images. This model was incorporated with prior knowledge of oil slicks and the algorithm managed to classify oil slicks with an accuracy of 94%. Manual inspections can be replaced by these types of algorithms when large ocean areas are to be inspected (Solberg et al., 2007).

Shu et al. (2010) have introduced another approach for automated dark-spot detection using SAR imagery. They have applied a spatial density feature to differentiate between dark spots and the background. Intensity threshold segmentation was used to identify possible dark spots and background pixels. Then the potential background pixels were removed using kernel density estimation, and then an area threshold and a contrast threshold were applied to eliminate any remaining false targets. Migliaccio et al. (2007) detect dark patches over SAR images using a polarimetric constant false alarm rate filter. Then the target decomposition theorem was applied to differentiate the oil spills and look-alikes.

Nirchio et al. (2005) developed a probabilistic method to distinguish oil spills from other similar sea surface features in SAR images using radiometric and geometric characteristics of the study area. They adopted automatic selection criteria to extract the potentially polluted areas from the images. Fiscella et al. (2000) also used a probabilistic approach to distinguish oil spills from similar

oceanic features. They have obtained physical and geometrical characteristics for both oil spills and other oceanic features from previously obtained measurements. Based on the results they have constructed a classification algorithm that demonstrated 80% accuracy on oil spill detection.

Most classification algorithms for oil spill detection are based on Bayesian or other statistically-based decisions. These are complex processes due to the many nonlinear and poorly understood factors involved (Frate et al., 2000). Frate et al. (2000) use a neural network approach to provide a classification algorithm to overcome their drawbacks and the neural net managed to discriminate over a set of independent examples between oil spills and look-alikes with a largely acceptable rate of success. Singha et al. (2013) also adopted Artificial Neural Networks (ANN) for oil spill detection. They have occupied two different ANNs to identify oil spills and to classify objectives into oil spills or look-alikes. This algorithm was validated with 91.6% accuracy for oil spills and 98.3% accuracy for look-alike situations. In addition, they established a new technique for edge detection and adaptive thresholding approaches. Garcia-Pineda et al. (2013) operated a Texture Classifier Neural Network Algorithm (TCNNA) to measure the spill's extent. Then they developed an oil emulation algorithm using TCNNA outputs to enhance the contrast of the oil slick. According to them, the detection was dependent on SAR incident angles and SAR beam mode configuration.

The use of SAR imagery to identify oil slicks in Sri Lanka is mostly limited to impact reports such as the UNEP and OCHA joint report on the X-Press Pearl maritime disaster by Partow et al. (2021). Kankanamge et al. (2022) attempted to identify the impacts of the X-Press Pearl incident using remote sensing techniques. However, they utilized Multispectral Landsat 8 satellite data to conduct their study (Kankanamge et al., 2022). Mahindapala (2020) used the Sentinel-1 SAR product to detect possible marine pollution by the tanker called "New Diamond", which caught fire on 3 September 2020 in the east of Sri Lanka. Pallewatta et al. (2023) and Anthony et al. (2023) use satellite images to estimate the extent of the oil slick from the MV X-Press Pearl incident, but they have focused on different aspects than the SAR image processing. This article only focused on one set of SAR imagery; temporal changes were not a concern.

With this background, the present article aims to detect the oil spill caused by the MV X-Press Pearl container ship on Sri Lanka's west coast from May to August 2021 using Sentinel-1 SAR data and measures the temporal changes of the oil slick.

Study area and the data used

Study Area

The X-Press Pearl ship was anchored in the Indian Ocean around 17 kilometers northwest of the Port of Colombo and 14 kilometers southwest of Negombo, Sri Lanka (Figure 1).

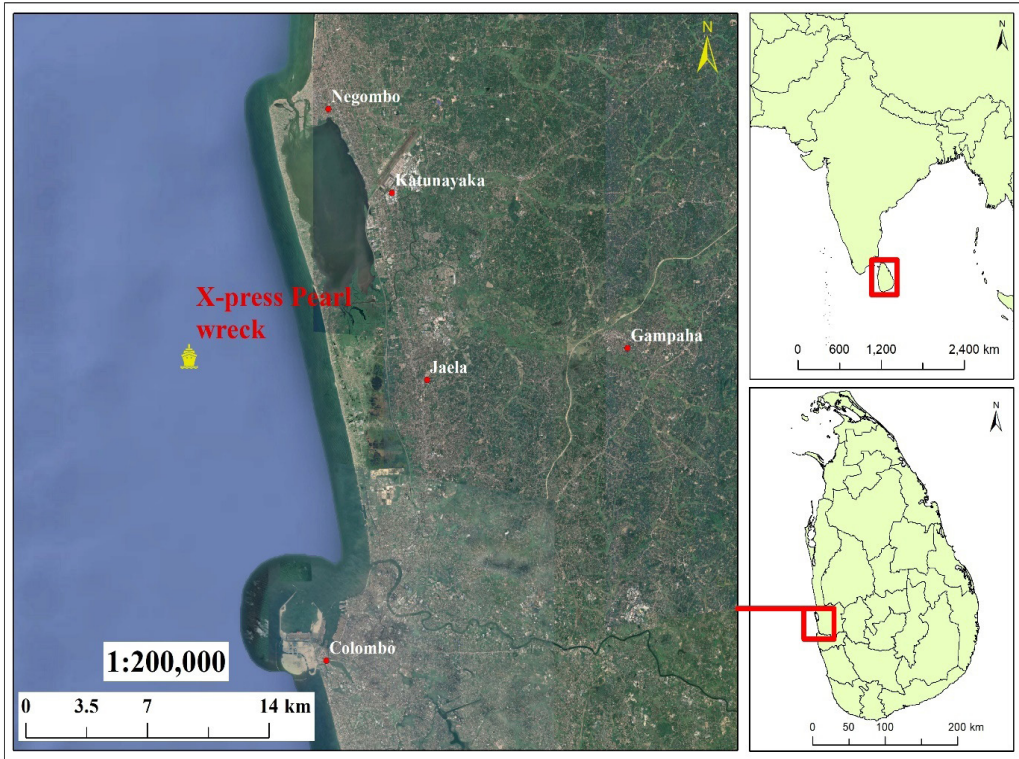


Figure 1: Location ($7^{\circ}04'57''\text{N}$ $79^{\circ}46'39''\text{E}$) of the X-Press Pearl wreck
(Source: Google Earth)

The direct distance to the shore from the site is around 8 kilometers and the approximate location of the wreck is $7^{\circ}04'57''\text{N}$ $79^{\circ}46'39''\text{E}$.

Materials

The C-SAR instrument of Sentinel-1 supports operation in dual polarization (HH+HV, VV+VH) implemented through one transmit chain (switchable to H or V) and two parallel receive chains for H and V polarization (EESA, n.d.). Therefore, Sentinel-1 (dual VV+VH polarization) data downloaded from the Copernicus open-access hub are used in this article (Table 1).

Table 1: Details of the used data from the Sentinel-1 satellite

Dataset and type	Acquired Date	Acquired time (UTC)
S1A_IW_GRDH_1SDV_0D76	08-June-2021	03:28:25
S1A_IW_GRDH_1SDV_C7DB	26-July-2021	02:15:05
S1A_IW_GRDH_1SDV_919F	31-August-2021	00:24:08

Methodology

In this article, visual and digital image processing techniques were applied and in the image processing, both single-band techniques and multi-band false color composites have been utilized. The methodology used is shown in Figure 2.

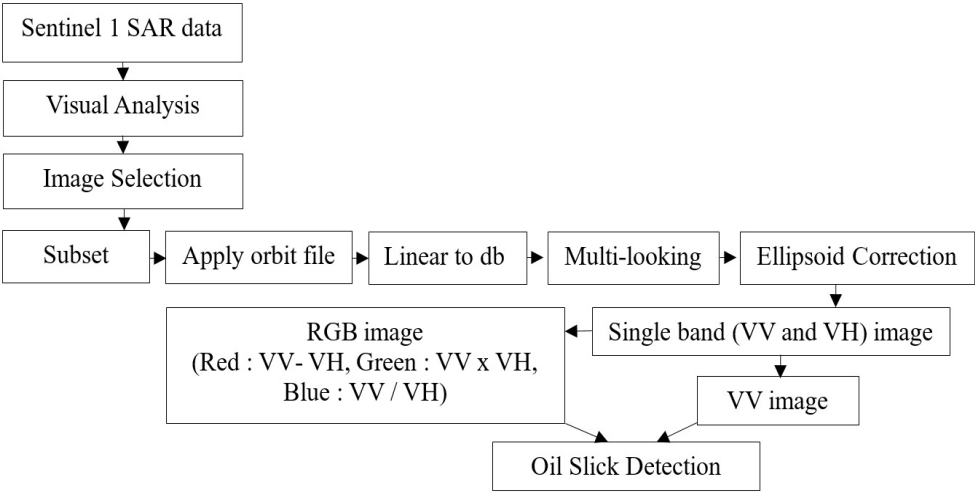


Figure 2: Diagram of the methodology used

Visual Analysis

Initially, nine SAR imageries, acquired on 27.05.2021, 08.06.2021, 13.06.2021, 02.07.2021, 14.07.2021, 26.07.2021, 07.08.2021, 19.08.2021 and 31.08.2021 from Sentinel-1, have been visually analyzed. Among those imageries, three datasets (Table 1) have been identified as images containing oil spills based on the classification (Figure 3) of Pavlakis et al. (2001).

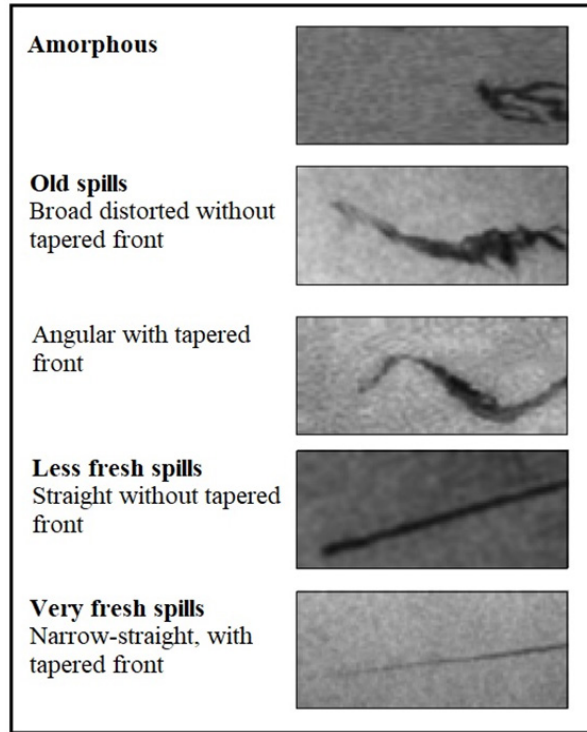


Figure 3: Spills classification in terms of their shapes
(Source: Pavlakis et al., 2001)

Image processing

Once the imageries were selected those images were processed using the Sentinel Application Platform (SNAP) (European Space Agency, n.d.). First, images were subset to the study area and then a precise orbit file was applied to get the accurate satellite position and velocity. Then the images were converted into decibels from linear and that improved the contrast and visualization of the images. Afterwards, those images were processed using the Multi-looking tool. Multi-looking is a technique that enhances the quality of the SAR image by diminishing the speckle (Hubert & Nahum, 2000) and this was applied to improve the images visually. Finally, ellipsoid correction was applied to correct the position and the orientation of the image. Both VV and VH polarization of these images have been processed.

Oil slick detection

Profile plots were derived using the possible oil slicks (dark region) from each image. Those profile plots were used to identify the reflectance over the ocean surface with the oil slick.

Apart from the single band analysis, false color representation was compiled using different band combinations. Afgatiani et al. (2022) have generated Sentinel-1 polarization composites to look for the best composites of Sentinel-1 polarization to visualize oil spills. They have tested several artificial band tests by modifying both VV and VH polarizations. The polarization applied in this research used “Subtract” (Equation 01) as the Blue band, “Multiple” (Equation 02) as the Green band, and “Divide” (Equation 03) as the Red band. Below are the equations used to create these bands.

Subtract	= $VV - VH$	As band one (1)
Multiple	= $VV \times VH$	As band two (2)
Divide	= VV / VH	As band three (3)

Results

Generally, there are three results: a single band VV polarization image, a profile plot of intensity value (dB), and a multi-polarization composite image.

During the initial visualizing stage, the Sentinel-1 VV and VH polarization images were explored with the SNAP software to identify dark regions within the study area. Images that were acquired on 8 June 2021, 26 July 2021, and 31 August 2021 have been identified with linear dark lines which are similar to the spill classification made by Pavlakis et al. (2001).

Profile plots are generated by processing in each VV band of three images taken by transect vertically. These profiles are plotting intensity values within pixels along the transects (Figures 4,5,6).

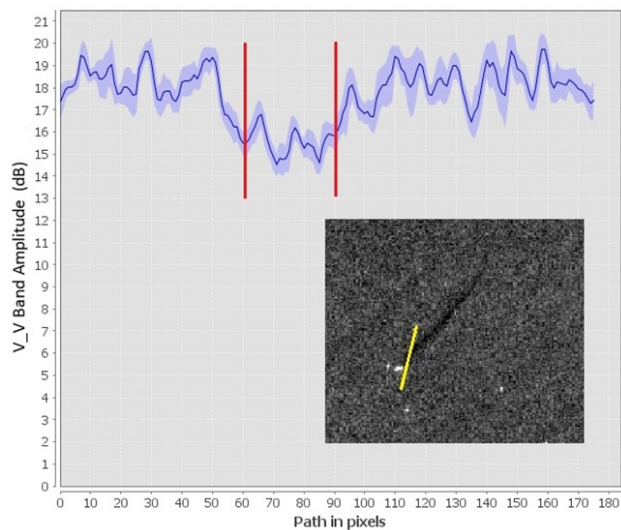


Figure 04: Profile plot of the VV band of 08.06.2021 image

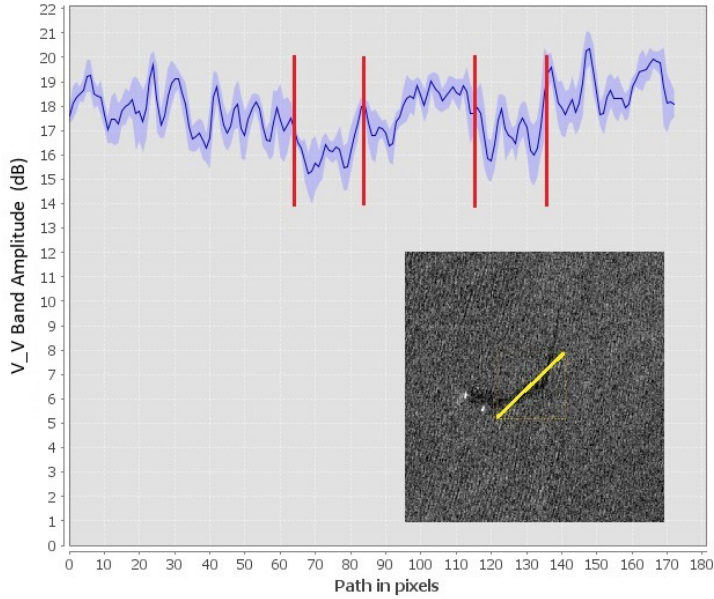


Figure 05: Profile plot of the VV band of 26.07.2021 image

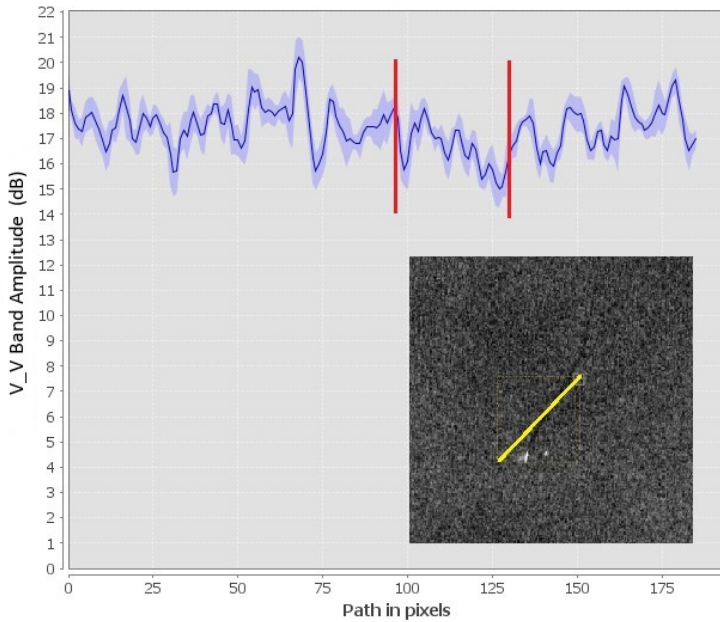


Figure 06: Profile plot of the VV band of 31.08.2021 image

The dark lines are visible in the VV polarization mode, but the VH mode does not have any dark lines. Once the processing was over, the VV mode provided a better understanding of the physical characteristics of oil spills (Figures 07(b), 08(d), and 09(f)).

False color composite images which are produced by compositing three bands (VV-VH, VVxVH, VV/VH) appear with unique colors for the land area (Green) and the ocean (Purple). However, the area with the oil slick appears as a dark region (Figures 07(a), 08(c), and 09(e)). This differentiates the sea surface and the oil slick.

Discussion

When considering the oil spill detection, the VV polarization of the SAR images shows a significant difference compared to the VH polarization. VV polarization shows the oil slicks as dark regions and therefore, those oil slicks can be identified within the initial visualization process. The oceanic region of the VH polarization appears as a dark region and therefore it is difficult to differentiate the oil slicks from the ocean. Therefore, VV polarization is the preferable polarization to detect oil spills and their behavior.

The fire and explosions that occurred on 25 May caused the containers to fall overboard. The Sentinel-1 image from 8 June 2021 indicates an oil slick (Figure 7).

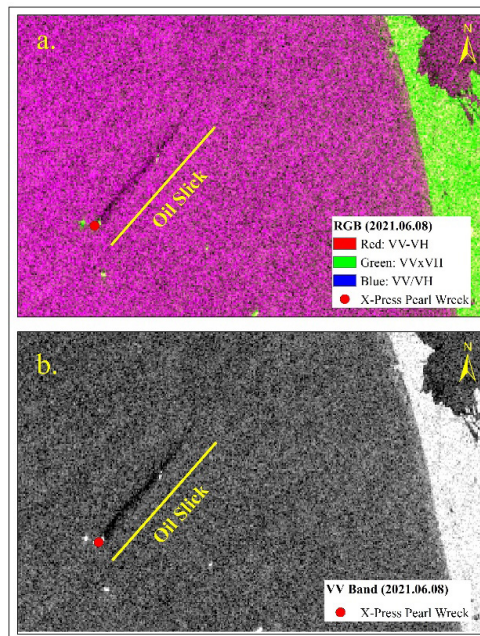


Figure 07: (a) RGB composite (b) VV mode of 08.06.2021 image

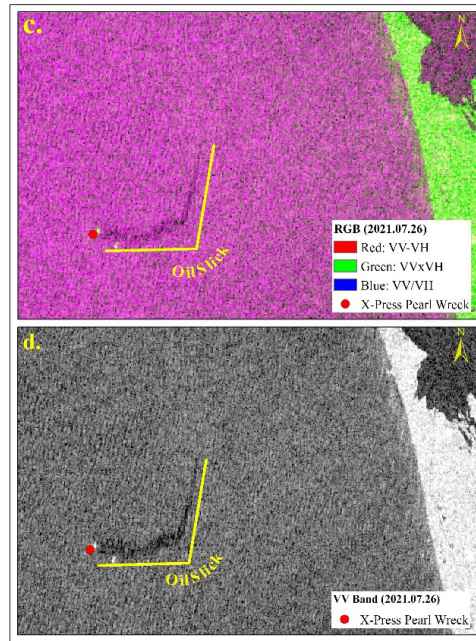


Figure 08: (c) RGB composite (d) VV mode of 26.07.2021 image

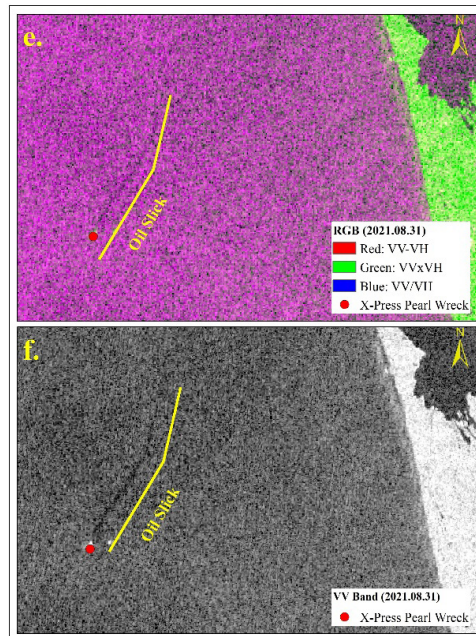


Figure 09: (e) RGB composite (f) VV mode of 31.08.2021 image

This fact is confirmed by the UNEP report (Partow et al., 2021). The length of this oil slick is 3.1 ± 0.012 km. According to the spill classification of Pavlakis et al. (2001), the respective oil spill can be classified as a “less fresh spill (Straight without tapered front)”. A spill representing detection a short time after discharge is defined as a less fresh spill. These types of spills tend towards high contrast (Pavlakis et al., 2001). The oil slick in this image shows more contrast compared to the other two images and therefore classifying this spill as a “less fresh spill” can be considered a reasonable judgment.

The next image which was captured on 26 July 2021 indicates an “L” shaped angular oil slick which is 3.6 ± 0.012 km in length. According to the spill classification of Pavlakis et al. (2001), the respective oil spill can be classified as an “angular with tapered front” oil slick. The general geometry of a spill will be distorted with the surface currents and wind fields (Pavlakis et al., 2001). These generate the angular shape of the slick. The final image, which was acquired on 31 August 2021, indicates a thin and linear shape with a slight angular oil slick. The length of the oil slick is 3.6 ± 0.012 km. This kind of oil slick is classified by Pavlakis et al. (2001) as a “very fresh spill (Narrow-straight, with the tapered front)”. Very fresh spills show weak backscattering (Pavlakis et al., 2001), and therefore those appear less frequently on SAR images.

By 31 August, three months had passed since the ship’s initial fire. The UNEP report by Partow et al. (2021) concluded that the continuous release of oil was flowing from the ship for nearly one month (8 June-4 July). However, with the results of this article, it is clear that the oil leakage has been continuing even after three months.

The brightness of the pixel intensity value varies based on the type of backscatter, such as spill-covered surfaces, sea levels, oil platforms, ships, etc. (Rao et al., 2022). The dampening effect due to the oil spill causes a low-intensity value compared to the surrounding surface (Afgatiani et al., 2022). The profile plots of these images show the low-intensity values of the region where the oil spill has been spread. The reflectance of the oil spill region of the 08.06.2021 image varies from 16.8 to 14.4 decibels with an average of 15.6 decibels while other regions have higher reflectance, ranging from 16.2 to 19.7 decibels with an average of 17.95 decibels of amplitude (Figure 4). The VV band of the 26.07.2021 image has two oil spill regions and those also record less reflectance, ranging from 15.1 to 17.9 decibels with an average of 16.5 decibels, whereas other regions record reflectance ranging from 16.2 to 20.1 decibels with an average of 18.15 decibels of intensity (Figure 5). The width of the oil slick from the 08.06.2021 image is low compared to the other oil slicks. Therefore, the oil spill region of the profile plot is narrow compared with the profile plots of the other images. However, the reflectance of the oil spill region of that image varies from 14.9 to 18.1 decibels

with an average of 16.5 decibels, and other regions indicate reflectance ranging from 15.7 to 20.1 decibels with an average of 17.9 decibels of amplitude (Figure 6).

The false color composite images made by combining VV-VH as the red band, VV x VH as the green band, and VV/VH as the blue band signify the oil slick by displaying the oil spill areas in black color. However, as a visual interpretation, compared to the single-band VV polarization images, it can be determined that these RGB composites are not capable of visualizing the oil spill region more precisely.

Conclusion

SAR images are more advantageous for cloud penetration and day and night data-acquiring abilities. These capabilities of the SAR images are useful during temporal analysis such as detecting oil spill regions on sea surfaces. The Singapore-flagged MV X-Press Pearl container ship which had on board toxic chemicals, plastics, and fuel was wrecked around 9 nautical miles northwest of the Port of Colombo in Sri Lanka in May 2021. With the release of plastics, chemicals, and oil to the marine environment, it became the worst marine environmental disaster in Sri Lanka. The Sentinel-1 SAR data detected the oil spills from the X-Press Pearl ship as dark lines with lengths of 3.1 ± 0.012 km for the image from 8 June and 3.6 ± 0.012 km for both images from 26 July and 31 August 2021. The analysis suggests that the VV polarization of Sentinel-1 has greater capability to identify these types of oil spills than the VH polarization. An oil spill causes a low-intensity value compared to the surrounding surface and that makes the regions with oil appear black. The results quantify the average intensity of the reflectance as 15.6, 16.5, and 16.5 decibels for the area covered with the oil slick and as 17.95, 20.1, and 17.9 decibels for other areas of the sea surface for the images acquired on 8 June, 26 July and 31 August 2021 respectively. In addition, this article suggests the single-band image is more capable of visualizing the oil spill than the multi-band false-color composite image. Even though the UNEP report concludes that the oil was flowing from the ship for nearly one month (8 June-4 July), what can finally be determined is that the oil was leaking into the ocean from the ship till the end of August 2021.

Conflict of interest

The author has no conflict of interest to declare.

References

- Afgatiani, P., Suhadha, A., & Ibrahim, A. (2022). The capability of Sentinel-1 polarization combinations for oil spill detection (study case: Karawang, Indonesia). *IOP Conf. Series: Earth and Environmental Science*. IOP Publishing. doi:10.1088/1755-1315/1109/1/012078
- Akkartal, A., & Sunar, F. (2008). The usage of Radar images in oil spill detection. *The International Archives of the Photogrammetry, Remote Sensing and Spatial Information Sciences*, 271-276.
- Alpers, W., Holt, B., & Zeng, K. (2017). Oil spill detection by imaging radars: Challenges and pitfalls. *Remote Sensing of Environment*, 133-147. doi:<https://doi.org/10.1016/j.rse.2017.09.002>
- Anthony, D., Siriwardana, H., Ashvini, S., Pallewatta, S., Samarasekara, S., Edirisinghe, S., & Vithanage, M. (2023). Trends in marine pollution mitigation technologies: Scientometric analysis of published literature (1990-2022). *Regional Studies in Marine Science*. doi:<https://doi.org/10.1016/j.rsma.2023.103156>
- Balogun, A., Yekeen, S., Pradhan, B., & Althuwaynee, O. (2020). Spatio-Temporal analysis of oil spill impact and recovery pattern of coastal vegetation and wetland using multispectral satellite Landsat 8-OLI imagery and machine learning models. *Remote Sensing*, 1225. doi:<https://doi.org/10.3390/rs12071225>
- Bonnington, A., Amani, M., & Ebrahimi, H. (2021). Oil Spill Detection Using Satellite Imagery. *Remote Sensing and Oceans*, 1-8. doi:10.21926/aeer.2104024
- Bozzi, C. (2021, July 09). *Could Sri Lanka's ship fire have been avoided? Here's what we can learn from the shocking disaster*. Retrieved from The Economic Times: <https://economictimes.indiatimes.com/news/international/world-news/could-sri-lankas-ship-fire-have-been-avoided-heres-what-we-can-learn-from-the-shocking-disaster/articleshow/84263605.cms>
- Chaturvedi, S., Banerjee, S., & Lele, S. (2020). An assessment of oil spill detection using Sentinel-1 SAR-C images. *Journal of Ocean Engineering and Science*, 116-135. doi:<https://doi.org/10.1016/j.joes.2019.09.004>
- EESA. (n.d.). *Sentinel Online, Instrument Payload*. Retrieved from EESA: <https://sentinels.copernicus.eu/web/sentinel/missions/sentinel-1/instrument-payload>
- Espedal, H. (2010). Satellite SAR oil spill detection using wind history information. *International Journal of Remote Sensing*, 49-65. doi:<https://doi.org/10.1080/014311699213596>
- Espedal, H., & Johannessen, O. (2000). Cover: Detection of oil spills near offshore installations using synthetic aperture radar (SAR). *International Journal of Remote Sensing*, 2141-2144. doi:<https://doi.org/10.1080/01431160050029468>

- European Space Agency;. (n.d.). *SNAP*. Retrieved from European Space Agency: <https://step.esa.int/main/toolboxes/snap/>
- Fiscella, B., Giancaspro, A., Nirchio, F., Pavese, P., & Trivero, P. (2000). Oil spill detection using marine SAR images. *International Journal of Remote Sensing*, 3561-3566. doi:<https://doi.org/10.1080/014311600750037589>
- Frate, F., Petrocchi, A., Lichtenegger, J., Calabresi, G., & Trivero, P. (2000). Neural Networks for Oil Spill Detection Using ERS-SAR Data. *Geoscience and Remote Sensing Symposium*, (pp. 2282-2287). doi:10.1109/IGARSS.1999.773451
- Garcia-Pineda, O., Macdonald, I., Hu, C., Svejksky, J., Hess, M., Dukhovskoy, D., & Morey, S. (2013). Detection of Floating Oil Anomalies From the Deepwater Horizon Oil Spill With Synthetic Aperture Radar. *Oceanography*, 124-137. doi:10.5670/oceanog.2013.38
- Hollinger, J., & Menella, R. (1984). Measurements of the distribution and volume of sea-surface oil spills using multifrequency microwave radiometry. In J.-M. Massin, *The NATO Committee on the Challenges of Modern Society*. Plenum Press.
- Hu, C., Lu, Y., Sun, S., & Liu, Y. (2021). Optical remote sensing of oil spills in the ocean : What is really possible? *Journal of Remote Sensing*. doi:10.34133/2021/9141902
- Hubert, C., & Nahum, C. (2000). *How to compute a Multi-Look SAR image?*
- Kankanamge, H., Senarathna, S., Jayawardhana, B., Bandara, D., & Madusankha, N. (2022). Oil spill maritime disaster management using remote sensing application; X-press pearl incident. *Young Scientists' Conference on Multidisciplinary Research-2022* (p. 54). Colombo: Young Scientists' Association, National Institute of Fundamental Studies, Sri Lanka.
- Kolokoussis, P., & Karathanassi, V. (2018). Oil spill detection and mapping using sentinel 2 imagery. *Journal of Marine Science and Engineering*, 2-12.
- Kubat, M., Holte, R., & Matwin, S. (1998). Machine learning for the detection of oil spills in satellite radar images. *Machine Learning*, 195-215.
- Mahindapala, W. (2020). Oil spill detection in the east of Sri Lanka with Sentinel-1 SAR. *The 1st JESSD Symposium*. doi:<https://doi.org/10.1051/e3sconf/202021102013>
- Marghany, M. (2023). *Recent Oil Spill Challenges That Require More Attention*. IntechOpen. doi:10.5772/intechopen.102299
- Maritime Executive. (2021). *Sri Lanka Seeks to Expedite Removal of X-Press Pearl*. Retrieved from The Maritime Executive: <https://maritime-executive.com/article/sri-lanka-seeks-to-expedite-removal-of-x-press-pearl>
- Martinez, A., & Moreno, V. (1996). An oil spill monitoring system based on SAR images. *Spill Science and Technology Bulletin*, 65-71.
- Migliaccio, M., Gambardella, A., & Tranfaglia, M. (2007). SAR Polarimetry to

- Observe Oil Spills. *IEEE Transactions on Geoscience and Remote Sensing*, 506-511. doi:10.1109/TGRS.2006.888097
- Natural resources, Canada. (2015, 11 24). *Oil Slick Detection*. Retrieved from Natural resources, Canada: <https://natural-resources.canada.ca/maps-tools-and-publications/satellite-imagery-and-air-photos/satellite-imagery-products/educational-resources/tutorial-radar-polarimetry/oil-slick-detection/9525>
- Nirchio, F., Tomaso, S., Biamino, W., Parisato, E., Trivero, P., & Giancaspro, A. (2005). Oil spills automatic detection from SAR images. *International Journal of Remote Sensing*, 26(6), 1157-1174. doi:10.1080/01431160512331326558
- NISAR. (n.d.). *Polarimetry*. Retrieved from NISAR, NASA-ISRO SAR Mission: <https://nisar.jpl.nasa.gov/mission/get-to-know-sar/polarimetry/>
- Pallewatta, S., Samarasekara, S., Rajapaksha, A., & Vithanage, M. (2023). Oil spill remediation by biochar derived from bio-energy industries with a pilot-scale approach during the X-Press Pearl maritime disaster. *Marine Pollution Bulletin*. doi:<https://doi.org/10.1016/j.marpolbul.2023.114813>
- Partow, H., Croix, L. C., Floch, L. S., & Alcaro, L. (2021). *X-Press Pearl maritime disaster, Sri Lanka ; Report of the UN environmental advisory Mission*. UNEP & OCHA. Retrieved 07 08, 2023, from <https://wedocs.unep.org/bitstream/handle/20.500.11822/36608/XPress.pdf>
- Pavlakakis, P., Tarchi, D., & Sieber, A. (2001). *On the monitoring of illicit vessel discharge, A reconnaissance study in the Mediterranean Sea*. Italy: European Commission.
- Perera, Kumudika;. (2021, June 7). *THE X-PRESS PEARL DEBACLE – EVENT FLOW*. Retrieved July 3, 2023, from Environmental Foundation: <https://efl.lk/x-press-event-flow/>
- Rao, V., Suneel, V., Raajvanshi, I., Alex, M., & Thomas, A. (2022). Year-to-year variability of oil pollution along the Eastern Arabian Sea: The impact of COVID-19 imposed lock-downs. *Marine Pollution Bulletin*.
- Roberto, L., & Giovanni, L. (2018). Oil Spill Detection Using Optical Sensors: A Multi Temporal Approach. *Satellite Oceanography and Meteorology*. doi:10.18063/som.v0i0.816
- Rubasinghe, C., Brosché, S., Withanage, H., Pathragoda, D., & Karlsson, T. (2022). *X-Press Pearl: A new kind of oil spill, A toxic mix of plastic and invisible chemicals*. Colombo: Centre for Environmental Justice (CEJ). Retrieved 07 08, 2023, from https://ipen.org/sites/default/files/documents/ipen-sri-lanka-ship-fire-v1_2aw-en.pdf
- Shirvany, R., Chabert, M., & Tournet, J. (2012). Ship and Oil-Spill Detection Using the Degree of Polarization in Linear and Hybrid/Compact Dual-Pol SAR. *IEEE Journal of Selected Topics in Applied Earth Observations and Remote Sensing*, 885-892.

- Shu, Y., Li, J., Yousif, H., & Gomes, G. (2010). Dark-spot detection from SAR intensity imagery with spatial density thresholding for oil-spill monitoring. *Remote Sensing of Environment*, 114(9), 2026-2035. doi:<https://doi.org/10.1016/j.rse.2010.04.009>
- Singha, S., Bellerby, T., & Trieschmann, O. (2013). Satellite Oil Spill Detection Using Artificial Neural Networks. *IEEE Journal of Selected Topics in Applied Earth Observations and Remote Sensing*, 2355-2363. doi:10.1109/JSTARS.2013.2251864
- Solberg, A., Brekke, C., & Husoy, P. (2007). Oil Spill Detection in Radarsat and Envisat SAR Images. *IEEE Transactions on Geoscience and Remote Sensing*, 746-755. doi:10.1109/TGRS.2006.887019
- Solberg, A., Stork, G., Solberg, R., & Volden, E. (1999). Automatic detection of oil spills in ERS SAR images. *IEEE Transactions on Geoscience and Remote Sensing*, 1916-1924. doi:10.1109/36.774704
- Topouzelis, K. (2008). Oil Spill Detection by SAR Images: Dark Formation Detection, Feature Extraction and Classification Algorithms. *Sensors*, 08(10), 6642-6659. doi:<https://doi.org/10.3390/s8106642>